Relativistic electron spectrum of ferromagnetic iron

1992 J. Phys.: Condens. Matter 4 497

(http://iopscience.iop.org/0953-8984/4/2/017)

J. Phys.: Condens. Matter 4 (1992) 497–503. Printed in the UK

Relativistic electron spectrum of ferromagnetic iron

S A Ostanin and V P Shirokovskii
Physics-Technical Institute, Academy of Sciences of USSR, Ural Branch,
132 Kirov Street, SU-426001, Izhevsk, USSR

Received 25 March 1991, in final form 31 July 1991

Abstract. The relativistic spin-polarized scheme of the electron spectrum calculation in crystal within the framework of the relativistic variant of the Korringa–Kohn–Rostoker method is realized. The technique proposed is used to calculate the electron bands and density of states of ferromagnetic iron. The crystallographic symmetry of the problem is investigated for the BCC lattice. The role of the exchange and spin–orbit interactions in forming the band structure of ferromagnetic iron are discussed.

1. Introduction

For a long time, calculations of the electron spectrum of ferromagnetic metals have been based on the Schrödinger equation of the form

$$[\Delta + (E - V - \Delta V \sigma_z)]\psi = 0 \tag{1}$$

(σ_z is the Pauli matrix). In such an approach the spin projection remains a 'good' quantum number and equation (1) divides into two scalar Schrödinger equations with the potentials depending on the sign of the spin projection:

$$V_{\pm} = V \pm \Delta V. \tag{2}$$

The crystallographic symmetry of the problem remains unchanged, and the resulting spectrum of a ferromagnet represents the superposition of the spectra of two Schrödinger problems with different potentials.

In recent years a number of papers have been devoted to constructing a consequent theoretical scheme of calculation of the electron states in collinear magnets based on the Dirac equation [1–3]. In the case of ferromagnets, this was realized in practice [4–8]. However, the conventional formalism for the scattering matrix results, in our view, in a complicated form of the dispersive equation.

We have developed a different, relatively simple technique for calculating the electron spectrum of a ferromagnet [9] within the framework of the relativistic version of the Korringa–Kohn–Rostoker method. The approach was based on the approximate equation for the large component ψ of the four-component Dirac spinor:

$$\Delta\psi + W[E - (V + \Delta V \sigma_z)]\psi - (W'/W)(\boldsymbol{\sigma} \cdot \hat{\boldsymbol{r}})(\boldsymbol{\sigma} \cdot \nabla)\psi = 0. \tag{3}$$

Here $\sigma_i (i = x, y, z)$ are the Pauli matrices, $\hat{\boldsymbol{r}}$ is the unit vector,

$$W = 1 + (E - V)/c^2 \tag{4}$$

c is the velocity of light, and the prime denotes the derivative with respect to r. The approximation consists in neglecting the term $\sigma_z \Delta V/c^2$ in (4).

0953-8984/92/020497 + 07 $03.50

In the present paper the technique proposed is used to investigate the electron spectrum of iron. Section 2 is devoted to the analysis of symmetry of equation (3) for a BCC lattice. The results of calculation of the electron spectrum and density of states obtained for ferromagnetic iron in the non-relativistic and relativistic variants of the technique are compared in section 3.

2. Symmetry of the problem

The point symmetry group of the crystalline Fe BCC lattice is the full cubic group O_h. Crystallographic symmetry of the problem induces symmetry in the quasi-momentum space; so the corresponding Brillouin zone (BZ) also has full cubic symmetry, the energy being invariant under all the 48 transformations that O_h consists of. This makes it possible to carry out calculations of the electron energy spectrum $E(k)$ in one forty-eighth of the BZ.

All the above holds true also in the non-relativistic variant (in the presence of ferromagnetic order). Taking into account relativistic effects, however, substantially changes the situation.

Since the scalar products $\boldsymbol{\sigma} \cdot \hat{\boldsymbol{r}}$ and $\boldsymbol{\sigma} \cdot \nabla$ involved in equation (3) remain unchanged upon any rotations and their product does not change upon inversion either, the last term in (3) has full cubic symmetry O_h for a BCC lattice. Therefore, the change in the symmetry of the problem is due only to the presence of the term $\sigma_z \Delta V$.

Obviously, the z-component of the spin remains unchanged upon rotations about the z axis (there are four such rotations in the group O_h); hence the following points are equivalent in the BZ:

$$(k_x, k_y, k_z) \qquad (\bar{k}_y, k_x, k_z) \qquad (\bar{k}_x, \bar{k}_y, k_z) \qquad (k_y, \bar{k}_x, k_z). \tag{5a}$$

The invariance of the spin under inversion adds four more points:

$$(\bar{k}_x, \bar{k}_y, \bar{k}_z) \qquad (k_y, \bar{k}_x, \bar{k}_z) \qquad (k_x, k_y, \bar{k}_z) \qquad (\bar{k}_y, k_x, \bar{k}_z). \tag{5b}$$

These are all just the transformations of the point group O_h, leaving equation (3) invariant.

In the absence of spin order the invariance of the Schrödinger equation under the time inversion operation $\hat{O}$ leads to the obvious conclusion that the states are doubly spin degenerate. In systems with magnetic order taken into account, time inversion is not so simple.

As the operator $\boldsymbol{\sigma}$ changes sign upon time inversion, with the product $(\boldsymbol{\sigma} \cdot \hat{\boldsymbol{r}})(\boldsymbol{\sigma} \cdot \nabla)$ remaining unchanged, the quantity $\sigma_z \Delta V$ should change sign too. This change in sign can be 'compensated' by means of rotation by π about an axis perpendicular to Oz, e.g. by rotation $\hat{C}_{2y}$ about the y axis. Thus, the product of the operations $\hat{C}_{2y}\hat{O}$ leaves equation (3) invariant and, taking into account the change in sign of the quasi-momentum upon time inversion, we get, from (5), eight more equivalent points in the BZ:

$$\begin{array}{llll} (k_x, \bar{k}_y, k_z) & (\bar{k}_y, \bar{k}_x, k_z) & (\bar{k}_x, k_y, k_z) & (k_y, \bar{k}_x, k_z) \\ (\bar{k}_x, k_y, \bar{k}_z) & (k_y, k_x, \bar{k}_z) & (k_x, \bar{k}_y, \bar{k}_z) & (\bar{k}_y, \bar{k}_x, k_z). \end{array} \tag{5c}$$

Table 1. The screening radii d_l of the model potential of ferromagnetic iron for two spin projections.

	$d_{l=0}$ (au)	$d_{l=1}$ (au)	$d_{l=2}$ (au)
Spin 'up'	0.720	0.755	0.700
Spin 'down'	0.720	0.730	0.675

3. Results of calculation of the ferromagnetic iron electron spectrum

To elucidate the role of relativistic effects in forming the electron structure of ferromagnetic iron we have carried out

(i) a non-relativistic calculation taking account of the spin polarization, i.e. using different potentials V_+ and V_- for the spins 'up' and 'down' (NRSP),

(ii) a conventional relativistic calculation for the same potentials V_+ and V_- (R) and

(iii) a consequent relativistic calculation taking account of the spin polarization within the scheme [9] (RSP).

The spectrum calculations have been performed by the Green function method [10] using an expansion in basis functions up to $l = 2$ at 125 k-points of one-sixteenth of the BZ. (This corresponds to 55 k-points in one forty-eighth of the BZ.) The spin was assumed to be z directed.

In our calculations we have used the l-dependent model potential which has inside the MT sphere the form [11]

$$V(r) = -(2/r)\{1 + (Z - 1)/H[\exp(r/d_1) - 1] + 1\} \tag{6}$$

($H = d_1(Z - 1)^{2/5}$, where d_1 is the screening radius of the l-type states). The choice of the parameter d_1 according to table 1 for the lattice constant $a = 5.4671$ au provides the value for the magnetic moment per atom of 2.2 μ_B.

The dispersion curves along the [010] direction of the BZ for the non-relativistic and relativistic versions of calculations are shown in figure 1 and figure 2(a) (the relativistic dispersive curves along the [001] direction near the Fermi energy E_F are shown in figure 2(b)). One can see that taking into account the relativistic effects together with the spin polarization leads to a qualitative change in spectrum—the complete removal of degeneracy occurring, in particular, at the highest-symmetry points of the BZ: Γ and H.

A general idea of the energy terms evolution in the above three approaches can also be given by table 2. We believe that it is necessary to provide only a minimum of numerical data, our RSP scheme being somewhat different from that proposed earlier [11–13]. As to the numerous data presented in [14] in graphical form, the comparison reveals no disagreement at all.

The results illustrating the influence of the crystalline field, relativistic effects and spin polarization on the energy spectrum are listed in table 3. The first three rows show E_F, the total width of the filled part of energy bands E_F–Γ_1, and the width of the filled part of d bands for either spin direction E_F–H_{min}. These quantities have been calculated only for the spin-polarized non-relativistic and relativistic variants of the theory, since the intermediate calculation with two different potentials has no physical meaning. The decrease in E_F observed when passing from the NRSP to RSP results from the total lowering

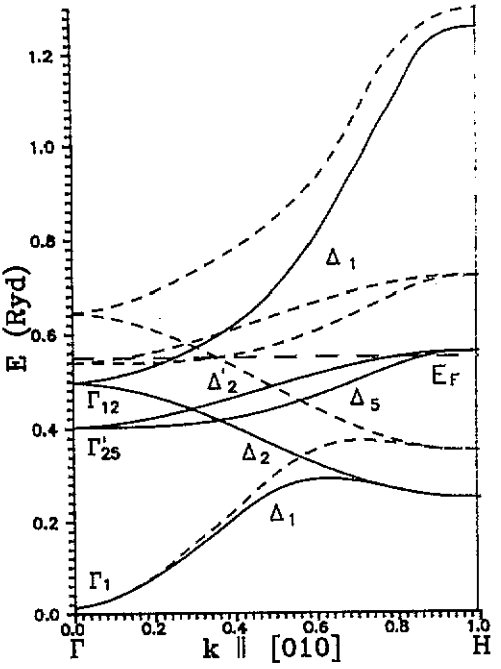

Figure 1. The non-relativistic spin-polarized band structure of iron along Γ–H [010] for the magnetic moment pointing along [001]: ——, states with spin 'up'; – – –, states with spin 'down'.

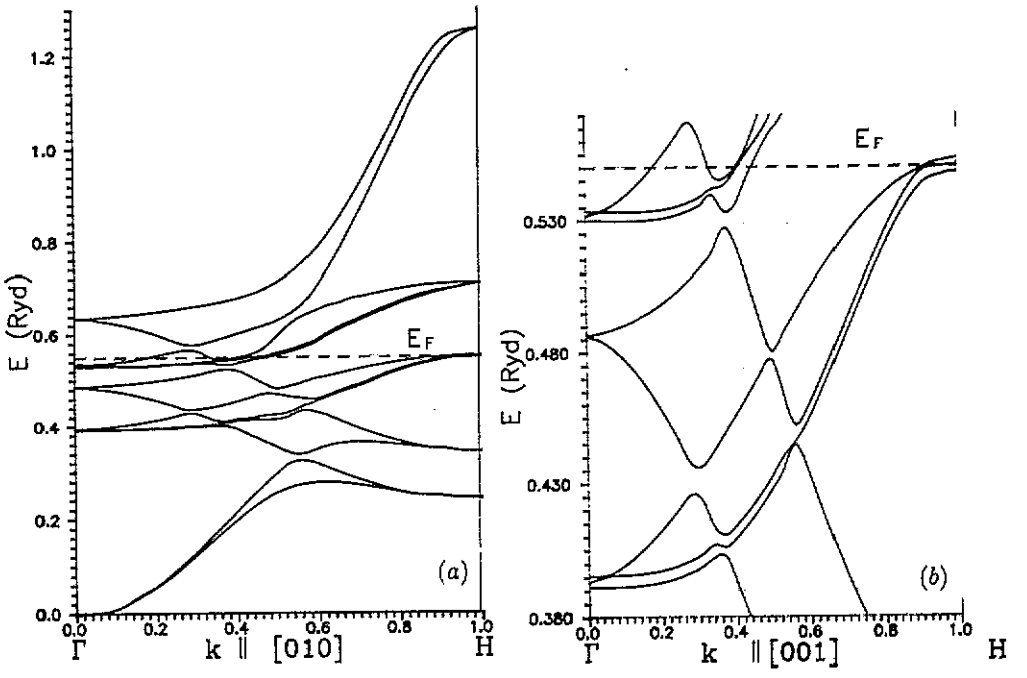

Figure 2. The relativistic spin-polarized band structure of iron (*a*) along Γ–H [010] for the magnetic moment pointing along [001] and (*b*) near the Fermi level along Γ–H [001] for the magnetic moment pointing along [001].

Table 2. The energy terms of iron in the non-relativistic spin-polarized (NRSP), relativistic (R) and relativistic spin-polarized (RSP) variants of calculation.

	Energy, NRSP (mRyd)			Energy, R (mRyd)		Energy, RSP (mRyd)	
	↑	↓		↑	↓	↑ ↓	↓ ↑
Γ'_{25}	402.4	539.6	$\Gamma^{(1)}_{8+}$	391.2	529.2	391.3	530.1
						393.3	531.3
			Γ_{7+}	398.0	535.6	395.7	533.8
Γ_{12}	496.9	645.1	$\Gamma^{(2)}_{8+}$	487.4	636.1	486.5	635.9
						487.2	636.0
H_{12}	248.5	351.9	$H^{(1)}_{8+}$	239.6	346.7	242.1	346.2
						242.2	346.3
H'_{25}	561.1	719.2	$H^{(2)}_{8+}$	547.9	706.6	547.9	706.5
						550.5	709.1
			H_{7+}	555.8	714.2	553.1	711.7

of the spectrum; the increase in E_F–Γ_1 and a small narrowing of E_F–H_{min} are due to a larger lowering of the s band than of the d bands. The above, which is a typical manifestation of the mass–velocity and Darwin effects which appear in relativistic theory, occurs upon the transition from the non-relativistic calculation to the relativistic calculation in the absence of spin polarization.

The next two rows illustrate the splitting of d states by the action of the crystalline field. One can see that taking into account the relativistic effects gives a negligible change in the splitting magnitude, particularly in the spin-polarized case. The same can be said about the exchange–correlation shift of the states with opposite spins (table 3, sixth to ninth rows).

In contrast, the magnitude of the spin–orbit splitting (which is rather small) is halved with the spin polarization taken into account as seen from the last two rows of table 3. This, together with the complete removal of degeneracy mentioned above, is the most important qualitative result of the analysis performed.

The density of states calculated through the spectrum obtained within the RSP scheme is plotted in figure 3 and agrees well with the plot given in [14]. It is essential to note, however, that all the main features of the curve in figure 3 are almost identical with those of the density-of-states plot based on the spectrum calculated within the NRSP approach. This is not surprising, since the changes in characteristic parameters of the energy band structure due to the transition from the NRSP to RSP variant are extremely small.

4. Conclusion

Summing up we should mention the changes in the electronic structure arising upon the transition from the non-relativistic spin-polarized version of the theory to the relativistic spin-polarized one, which are expected to be revealed by experiment.

First, the changes occurring in the energy spectrum structure near the Fermi level and hybridization of states with opposite spins are certain to alter the nature of the

Table 3. The changes in energy spectrum characteristics in the non-relativistic spin-polarized (NRSP), relativistic (R) and relativistic spin-polarized (RSP) variants of calculation.

	Energy change, NRSP (mRyd)			Energy change, R (mRyd)		Energy change, RSP (mRyd)	
	↑	↓		↑	↓	↑ ↓	↓ ↑
E_F		558				550	
E_F–Γ_1		548				557	
E_F–H_{min}	310	206					
Γ_{12}–Γ'_{25}	94					306	205
H'_{25}–H_{12}	313	106	$\Gamma^{(2)}_{8+}$–$\Gamma^{(1)}_{8+}$	96	107	95	
		367	H_{7+}–$H^{(1)}_{8+}$	316	368	308	106
$\Gamma'_{25}\downarrow$–$\Gamma'_{25}\uparrow$		137	$\Gamma^{(1)}_{8+}\downarrow$–$L^{(1)}_{8+}\uparrow$				364
$\Gamma_{12}\downarrow$–$\Gamma_{12}\uparrow$		148	$\Gamma^{(2)}_{8+}\downarrow$–$\Gamma^{(2)}_{8+}\uparrow$		138		
$H_{12}\downarrow$–$H_{12}\uparrow$		103	$H^{(1)}_{8+}\downarrow$–$H^{(1)}_{8+}\uparrow$		149		139
$H'_{25}\downarrow$–$H'_{25}\uparrow$		158	$H^{(2)}_{8+}\downarrow$–$H^{(2)}_{8+}\uparrow$		104		150
					158		101
			Γ_{7+}–$\Gamma^{(1)}_{8+}$	7			157
			H_{7+}–$H^{(2)}_{8+}$	8	6	4	
					8	5	3
							5

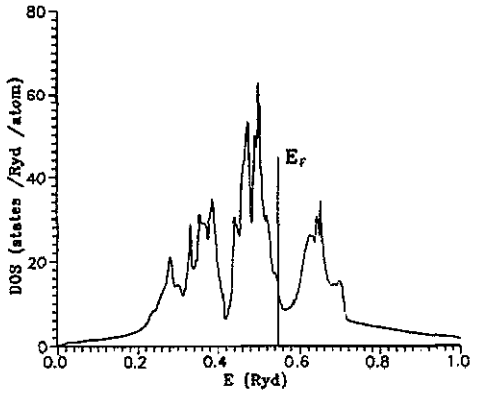

Figure 3. The total density of states for ferromagnetic iron with the magnetization along [001]

optical absorption in the energy range up to 1 eV. In fact, this has already been revealed by experiment [12] and confirmed by theory [13], although a more rigorous calculation would be useful.

Second, a change in the Fermi surface topology may be revealed when studying the oscillation effects which calls for a detailed calculation of the Fermi surface geometry in the relativistic spin-polarized scheme. Up to now, experiments have been interpreted within the framework of the non-relativistic theory [14].

Third, one can expect to detect a difference in size between separate cross sections of the Fermi surface along the equivalent crystallographic directions differently oriented with respect to the magnetization axis, which occurs in the relativistic version of the theory [14].

References

[1] Feder R, Rosicky F and Ackermann B 1983 *Z. Phys.* B **52** 31
[2] Strange P, Staunton J B and Gyorffy B L 1984 *J. Phys. C: Solid State Phys.* **17** 3355
[3] Shadler G, Weinberger P, Boring A M and Albers R C 1986 *Phys. Rev.* B **34** 713
[4] Strange P, Ebert H, Staunton J B and Gyorffy B L 1989 *J. Phys.: Condens. Matter* **1** 2959
[5] Strange P, Ebert H, Staunton J B and Gyorffy B L 1989 *J. Phys.: Condens. Matter* **1** 3947
[6] Krutzen B C H and Springelkamp F 1989 *J. Phys.: Condens. Matter* **1** 8369
[7] Ebert H 1988 *Phys. Rev.* B **38** 9390
[8] Matsumoto M, Staunton J B and Strange P 1991 *J. Phys.: Condens. Matter* **3** 1453
[9] Ostanin S A and Shirokovskii V P 1990 *J. Phys.: Condens. Matter* **2** 7585
[10] Segall B and Ham F S 1968 *Methods of Computational Physics* vol 8 (New York: Academic) p 251
[11] Green A E S, Sellin D D and Zachor A S 1969 *Phys. Rev.* **184** 1
[12] Shirokovskii V P, Kirillova M M and Shilkova N A 1982 *Zh. Exp. Teor. Fiz.* **82** 784
[13] Halilov S V and Uspenskii Yu A 1990 *J. Phys.: Condens. Matter* **2** 6137
[14] Johnson W B, Anderson J R and Papaconstantopoulos D A 1984 *Phys. Rev.* B **29** 5337